

## H $\alpha$ Distance Constraints for High Velocity Clouds in the Galactic Halo

Joss Bland-Hawthorn

*Anglo-Australian Observatory, PO Box 296, Epping, NSW 2121, Australia*

Philip R. Maloney

*Center for Astrophysics & Space Astronomy, University of Colorado, Boulder, CO 80309-0389*

**Abstract.** We present some developments in determining H $\alpha$  distances to high-velocity clouds (HVCs) in the Galactic halo. Until recently, it was difficult to assess the nature and origin of HVCs because so little was known about them. But now several HVCs have reliable distance bounds derived from the stellar absorption technique, and more than a dozen have abundance measurements. In addition, twenty or more HVCs have been detected in H $\alpha$  (and a few in optical forbidden lines). Over the past five years, we have been developing a model of the halo radiation field which includes contributions from the stellar disk, the stellar bulge, the hot corona, and the Magellanic Clouds.<sup>1</sup> In certain instances, the H $\alpha$  flux from an opaque H I cloud can be used to derive a crude distance constraint to the cloud. For a UV escape fraction of  $\hat{f}_{\text{esc}} \approx 6\%$  perpendicular to the disk ( $f_{\text{esc}} \approx 1 - 2\%$  when averaged over solid angle), the HVCs appear to be broadly consistent with the spiral arm model. We caution that a larger database with full sky coverage is required before the usefulness of H $\alpha$  distances can be fully assessed. We present a number of detailed predictions from our distance frame to encourage independent assessments from future observations. If the model is valid, we find that most HVCs detected to date are scattered throughout the halo up to distances of 50 kpc from the Sun. Most of this material is likely to be debris from recent galaxy interactions, or even debris dislodged from the outer Galaxy disk. We propose some future tests of the H $\alpha$  distance model and briefly discuss recent H $\alpha$  detections along the Magellanic Bridge and Magellanic Stream.

### 1. Introduction

Observations of the Galactic halo make a compelling case that the formation of halos continues to the present day (Wyse 1999). The halo appears to have built

---

<sup>1</sup>The `diskhalo` ionization code, along with full documentation (Bland-Hawthorn & Maloney 2001), is to be made available for general use.

up through a process of accretion and merging of low-mass structures which is still going on at a low level. Hierarchical cold dark matter (CDM) simulations, however, predict that the Galactic halo should have many more satellites than are actually observed (Klypin et al. 1999; Moore et al. 1999).

As much as 40% of the sky is peppered with high-velocity HI clouds (HVCs) which do not conform to orderly Galactic rotation (Wakker & van Woerden 1991; Putman 2000). These are interesting accretion candidates – particularly if they are associated with dark matter ‘mini halos’ – except that their distances,  $d$ , are unknown for all but a few sources. As a result, fundamental physical quantities – size ( $\propto d$ ) and mass ( $\propto d^2$ ) – are unconstrained which has encouraged wide speculation as to the nature of HVCs (Wakker & van Woerden 1997).

Indeed, the current renaissance in HVC studies can be traced in part to an interesting suggestion by Blitz et al. (1999). They showed that the velocity centroids and groupings of positive/negative velocity clouds on the sky may be understood within a reference frame centered on the Local Group barycenter (*cf.* Zwaan & Briggs 2000). They interpret HVCs as gas clouds accreting onto the Local Group over a megaparsec sphere. Braun & Burton (2000) identify specific examples of compact clouds that have ‘rotation curves’ consistent with CDM mass profiles. For sources at 700 kpc, the kinematic signatures imply a high dark-to-visible mass ratio of 10–50.

This paper addresses the distance problem. In earlier papers (*e.g.*, Bland-Hawthorn et al. 1998; Bland-Hawthorn & Maloney 1999 – BM99), we showed that faint H $\alpha$  measures from distant HI clouds could, in principle, be used to estimate crude distances to the clouds. The H $\alpha$  emission measure from any cloud which can be detected at 21 cm is a direct measure of the Lyc (Lyman continuum) radiation field, independent of distance. In order to interpret the H $\alpha$  emission, we require a realistic model of the Galactic halo ionizing field. Here, we present some recent developments in deriving H $\alpha$  distances which significantly extends our earlier work.

## 2. The Escape of UV radiation from the Galaxy

Since we have discussed the UV escape fraction ( $\hat{f}_{\text{esc}}$ ) from the Galaxy at length in earlier articles (*q.v.*, Bland-Hawthorn & Putman 2001), only a short discussion is given here. The likely value of  $\hat{f}_{\text{esc}}$  is still uncertain but there is increasing evidence that UV does radiate far from HII regions. To cite one of several recent demonstrations, the warm (diffuse) ionized medium in external galaxies clearly shows the hallmark of the HII regions even after these have been masked out of the H $\alpha$  image (*e.g.*, Zurita et al. 2001; Cianci 2001).

Further evidence that UV must escape the Galaxy comes from the measured electron density profile from halo pulsars. Manchester & Taylor (2000; see also Nordgren, Cordes & Terzian 1992) have modelled this with a scale height of 800 pc which exceeds or is comparable to the scale height of the diffuse HI (warm neutral medium; Lockman 1984). Without fine-tuning, it is unlikely that the Reynolds layer represents a radiation-bounded medium within a co-extensive HI envelope. We know that the radiation field must be soft from the weakness of HeI $\lambda$ 5876 and non-detection of [HeII] $\lambda$ 4686 (Reynolds & Tufte 1995). Furthermore, the observed weakness of [OI] $\lambda$ 6300/H $\alpha$  indicates two things: (i)

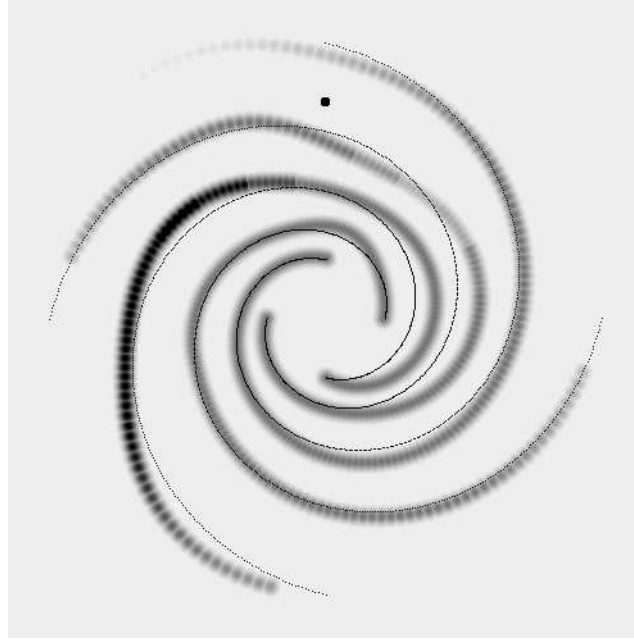


Figure 1. The spiral arm distribution of UV emitting sources used in the `diskhalo` ionization code where the dot shows the Sun’s position. The model is identical to the Taylor-Cordes density distribution in the near field ( $r < 10$  kpc). In the far field, the spiral arms are forced to follow the Ortiz-Lepine model shown as continuous lines.

the ionization fraction must be high (Reynolds 1989), (ii) all of the UV photons produced in the disk cannot be absorbed in radiation-bounded HII regions (Domgörgen & Mathis 1994).

It is important to appreciate that the Fabry-Perot ‘staring’ method is so sensitive that we only need  $f_{\text{esc}} \sim 1\%$  for the H $\alpha$  distance method to be useful. In fact, our preliminary analysis of H $\alpha$  levels from HI clouds with stellar distance brackets suggests that indeed  $f_{\text{esc}} \approx 1\text{--}2\%$  (see § 6). At distances of 300 kpc along the polar axis, the Galaxy field is comparable to the cosmic UV field. The expected H $\alpha$  levels are of order 1 – 2 mR and it may be possible to reach these levels<sup>2</sup> with new differential techniques (*e.g.*, Glazebrook & Bland-Hawthorn 2001).

### 3. The importance of spiral arms

Our early attempts to derive H $\alpha$  distances made use of a smooth exponential distribution of ionizing sources (BM99). For HVC distances within 10 kpc of the plane, we need a more realistic distribution of ionizing sources than the exponential disk model. This would be straightforward if we knew the exact location of all O stars, and the precise dust distribution throughout the Galaxy.

---

<sup>2</sup>1 milliRayleigh =  $10^3/4\pi$  phot cm<sup>-2</sup> s<sup>-1</sup> sr<sup>-1</sup> =  $2.4 \times 10^{-10}$  erg cm<sup>-2</sup> s<sup>-1</sup> sr<sup>-1</sup> at H $\alpha$ .

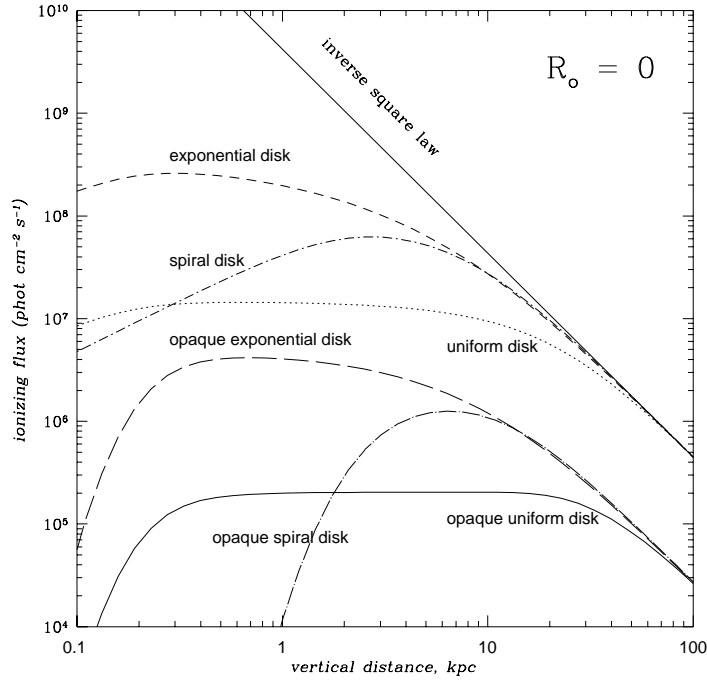


Figure 2. A comparison of the halo ionizing flux for different disk distributions (uniform emissivity, exponential and spiral) within the `diskhalo` code compared to a simple inverse square law. The vertical distance is measured from the center of the disk along the polar axis. The top three curves are in the absence of dust and converge in the far field limit. The lower three curves include the effects of dust where  $\tau_{LL} = 2.8$ .

But this will not be possible until the GAIA astrometric mission flies in 2010. However, most studies of spirality in the Galaxy agree that the tangent points of the spiral arms are well defined over a wide range of methods and wavelengths, in particular, the distribution of pulsar dispersion measures with galactic longitude (Taylor & Cordes 1993).

For this reason, the non-axisymmetric component of the **diskhalo** ionization model links its fortunes to the standard model for determining pulsar distances. Rough distances to pulsars are deduced from the dispersion (and scattering) measure due to warm electrons along the line of sight. Early attempts used a smooth distribution of electrons (*e.g.*, Manchester & Taylor 1981) although Lyne, Manchester & Taylor (1985) showed that typical distance estimates have random errors as large as a factor of two. After the inclusion of smooth spiral arms, Taylor & Cordes (1993) predict that most distances should be good to  $\sim 20\%$ . This level of accuracy is somewhat surprising when one examines face-on spirals in the Ultraviolet Imaging Telescope (UIT) database. But the distance model is largely borne out by lower limits derived from pulsar sight lines which show H I in absorption.

#### 4. Stellar bulge contribution

A component largely overlooked to date is the UV field arising from the Galactic spheroid (O’Connell 1999). A ‘UV upturn’ component is now well established for ellipticals and S0s (Greggio & Renzini 1999; Macchetto et al. 1996; Bica et al. 1996). Binette et al. (1994) suggest this may arise from post-AGB stars evolving from an old stellar population. A rough estimate is  $7 \times 10^{50} (M_{\text{bulge}}/10^{10} M_{\odot})$  ionizing phot s $^{-1}$ .  $M_{\text{bulge}}$  is the mass of the Galactic halo bulge which is uncertain to a factor of two, *i.e.*,  $M_{\text{bulge}} \approx 1 - 2 \times 10^{10} M_{\odot}$  (Dwek et al. 1995; Zhao 1996). Since much of the bulge stars lie outside most of the absorbing ISM, the UV flux which escapes into the halo may be non-negligible and more smoothly distributed compared to flux which escapes the disk. When a bulge component is discussed below, we include an isothermal distribution of sources with a total luminosity of  $7 \times 10^{50}$  phot s $^{-1}$ . We assume that all of the UV escapes, although the dusty disk blocks half of the radiation. The hot corona component is discussed in BM99. Both sources of UV are examined briefly in the next section.

#### 5. The disk-halo ionization model

The **diskhalo** model includes five basic components: the spiral arm (or exponential) disk defined by the OB star population; stellar bulge; hot coronal halo; LMC (and SMC); cosmic background. In addition, the resulting radiation field can be moderated by the presence of a plane parallel opacity law, and projected H $\alpha$  emission measures can be derived with a variety of schemes.

In Fig. 1, we show how the spiral arms are represented in the ionization model. In the near field ( $r < 10$  kpc), the distribution is essentially identical to the Taylor-Cordes model. However, the spiral arms are incomplete on the far side of the Galaxy which required us to extend the arm coverage by 60%. This

was done by splicing the Taylor-Cordes model onto the basic model parameters of Ortiz & Lepine (1993). The spiral arms cover a total area of  $100 \text{ kpc}^2$  within a circle with 12 kpc radius, compared with the exponential model which extends out to a radius of 25 kpc (although most of the emissivity lies within a 12 kpc radius).

The `diskhalo` manual (Bland-Hawthorn & Maloney 2001) describes how the electron density field is inverted to produce the surface density of ionizing photons. Fig. 2 shows how the three different disk distributions compare as we approach the disk along the polar axis of the Galaxy. Fig. 3 presents a cross section through the halo field and shows that the form of the dusty spiral is very different to that of the exponential disk within 10 kpc, which can also be seen in Fig. 2.

An important prediction of the spiral arm and the exponential models is that ionizing flux seen by a cloud ‘inside’ the Solar Circle should be much higher than the flux seen by a cloud on the ‘outside’. We have tried to illustrate this effect in Fig. 4. For this trend to be evident, a large nearby sample of clouds is required over a wide solid angle. One possible population which might reveal this effect are the intermediate velocity clouds (IVCs). In the next section, we show the prediction for one such cloud, Complex K.

Fig. 4 shows how a stellar UV bulge (or, for that matter, a hot UV corona) can wash out some of the contrast produced by spiral arms (see also Fig. 8). The presence of a UV-bright stellar bulge can remove the near-field solution which typically arises with the spiral arm models. This phenomenon is seen in the exponential disk predictions in Fig. 5. The hot galactic corona is not as effective as the stellar bulge at washing out the spiral structure since, even though it has a scale length a factor of 5 larger than the bulge, the expected flux levels are lower by about the same factor.

## 6. Predicted $\text{H}\alpha$ distances to $\text{H}\text{I}$ clouds

Here we present predictions for HVCs with measured  $\text{H}\alpha$  fluxes. We emphasize that the method is only intended as a statistical constraint. Even with large numbers of  $\text{H}\alpha$  detections for each cloud complex, it may only be useful to within a factor of a few and even this level of confidence needs to be tested.

We used the `diskhalo` code with the dusty spiral disk ( $\tau_{LL}=2.8$ ). We use a conservative model with a hot corona but no stellar bulge component. The choice of  $\tau_{LL}$  is discussed in detail elsewhere but largely arises from the WHAM detections of Complexes A, C, K and M (see below). Weiner et al. (2001, these proceedings) derive a similar value from an analysis of their own observations. Since galactic coordinates have not yet been published for some of the detections, we have averaged our calculations over the observed  $\text{H}\text{I}$ .

A major benefit of the spiral arm model is the order of magnitude larger contrast in  $\text{H}\alpha$  that one obtains compared to the exponential disk model. A good example of this comes from the Complex L sight line presented in Fig. 5. This cloud is found to be very bright in  $\text{H}\alpha$  by both the Las Campanas (Weiner et al. 2001) and TAURUS teams (Putman et al. 2001, in prep.). The exponential model fails by a large factor to explain the signal whereas this is a natural consequence of the spiral arm model if the complex is 1 kpc from the disk,

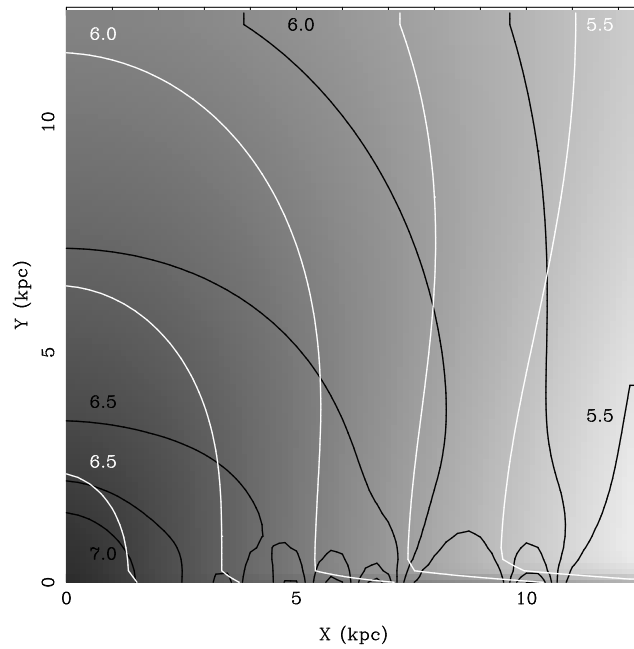


Figure 3. A cross section through the halo field produced by the **diskhalo** model for two cases: the dusty exponential disk (white contours and halftone) and the dusty spiral disk (black contours). The Galactic Center is at (0,0). The numbers give the ionizing flux in units of  $\log(\text{phot cm}^{-2} \text{ s}^{-1})$ .

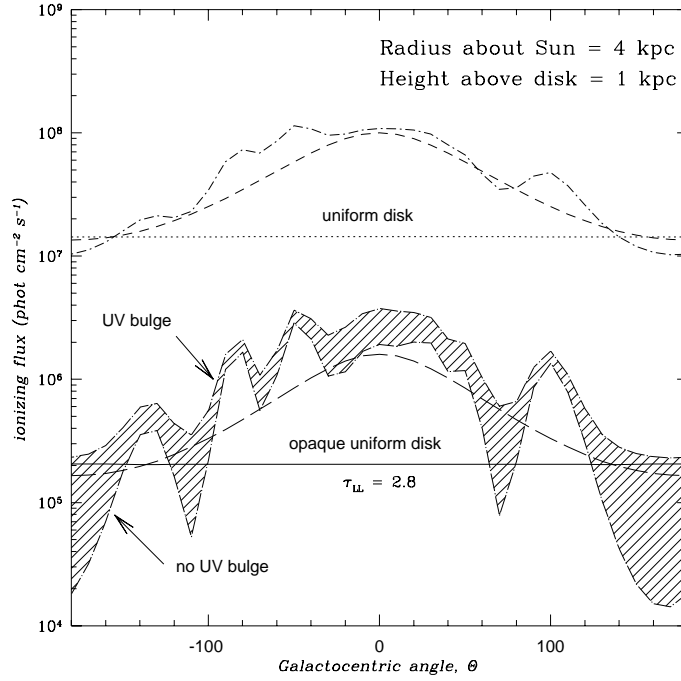


Figure 4. The predicted ionizing flux around a ring at 1 kpc elevation with a radius of 4 kpc centered on the Sun ( $\Theta = 0$  is towards the Galactic Center). The upper curves show the flux for optically thin cases ( $\tau_{LL} = 0$ ) of a uniform, exponential and spiral disk; the lower curves are for the dusty models ( $\tau_{LL} = 2.8$ ) of the same. The dusty spiral disk has been computed with and without the presence of a stellar UV bulge. The expected flux levels are much higher in the direction of the Galactic Center ('inside') compared to the Anti-Center ('outside').



in which case the cloud system lies directly above a spiral arm. Independent support for this comes from the observation by both teams that the [NII]/H $\alpha$  ratios are very elevated in this system, an effect seen at low latitudes in external edge-on galaxies. The same temperature effect (Reynolds, Haffner & Tufte 1999) is seen in the Smith Cloud which is also thought to lie within a few kpc of the disk (see below).

But the contrast effect comes at a price. For most of the modelled sight lines in Fig. 5, there is a near-field and a far-field prediction. This is because in almost any direction away from the Sun, the radius vector crosses a spiral arm. Multiple solutions are generally avoided at latitudes higher than  $20^\circ$  because as we move away from the disk, the details of the distribution become less important. An example is the Smith Cloud (GCP) discussed in Bland-Hawthorn et al. (1998). This cloud is predicted to lie at 1 kpc or roughly 15 kpc. Two of the sight lines (Complex L, Co-Rotate) are multiple valued for the observed H $\alpha$ .

The WHAM detections of Complexes A, M and C are also modelled in Fig. 5. These clouds are particularly important as they have distance bounds from the stellar absorption line (SAL) method. If a star of known distance lies beyond the cloud, and another star of known distance falls in front, we obtain a distance bracket for the cloud if it is seen in absorption against the distant star, but not in the nearer star. Complex M (specifically, Cloud MII) has an upper limit of 4 kpc on its distance (Ryans et al. 1997); no lower bound exists. The far-field limit is only consistent at the  $1.3\sigma$  level. Complex A lies between 4 and 10 kpc from the Sun (van Woerden et al. 1999) which appears consistent with the far field limit. There is a suggestion that this range could be tightened to 8 and 10 kpc should the complex not be detected on the spectrum of PG 0832+675, in which case the far field prediction is a factor of two too small. Complex C has a secure lower limit on its distance of 1 kpc, based upon five stellar probes; a much weaker limit of  $>6$  kpc is provided by the non-detection of the cloud in BS 16034-0114 (Wakker 2001). Both near- and far-field solutions are consistent with a firm distance limit ( $>1$  kpc); only the far-field solution is consistent with the weaker limit ( $>6$  kpc).

The WHAM team have recently published H $\alpha$  observations for the IVC Complex K (Haffner et al. 2001). There is little absorption line data in this direction although the cloud does appear to lie between 0.3 and 7.7 kpc. The sight line to Complex K lies directly over the tangent point of a spiral arm which explains the broad distribution in Fig. 5. The WHAM team present three averaged H $\alpha$  measurements for this cloud. In the absence of a characteristic H $\alpha$  measurement for a fully mapped cloud, we take the peak H $\alpha$  detection towards the center of a cloud as the most important for distance determination.<sup>3</sup> The brighter detections are entirely consistent with the SAL bounds, although the weaker detections would push the far-field limit out to 10 kpc or more.

---

<sup>3</sup>This emphasizes a weakness in the H $\alpha$  method – see Bland-Hawthorn & Maloney 1999b for a detailed discussion – in that a detailed mapping is normally required to reliably interpret what part of the cloud is being lit up in H $\alpha$ . However, this is not always a problem. Weiner et al. (2001, these proceedings) and Tufte et al. (1998) find that the internal H $\alpha$  dispersion in a significant number of HVCs can be small.

In summary, for HVCs with well defined distance bounds, we find (see also Weiner et al. 2001) that the observed  $H\alpha$  is roughly consistent with  $\hat{f}_{\text{esc}} \approx 6\%$  ( $\tau_{LL} = 2.8$ ) although the present uncertainties are about a factor of 2. Note that this escape value  $\hat{f}_{\text{esc}}$  is defined orthogonally to the disk plane; the solid-angle averaged value is  $f_{\text{esc}} \approx 1\text{--}2\%$ .

Finally, the Las Campanas team (Weiner et al. 2001) have achieved some faint detections to clouds which are thought to be farther afield. We show the predictions for three of these (Co-Rotate, GCN and Population N). We have run the code for all HVCs with  $H\alpha$  detections to date. Population N appears to lie at the greatest distance (30–45 kpc) if the  $H\alpha$  emission arises from the disk radiation field.

## 7. The Magellanic System

The LMC has several highly active star forming regions, particularly regions of very recent star formation (Shapley III) and of ongoing star formation (30 Doradus). The basic ionizing requirement of the LMC from combined UV, optical and radio studies appears to be  $5 \times 10^{51} \text{ phot cm}^{-2} \text{ s}^{-1}$ . Within a factor of two, this is consistent with OB star counts (Walborn 1984; Parker 1993), radio continuum observations (McGee, Brooks & Batchelor 1972; Israel & Koornneef 1979), and vacuum ultraviolet observations (Smith et al. 1987) of the LMC. However, the total number of ionizing photons produced by the LMC HII regions, spread over a 5 kpc region, may be as high as  $1.5 - 3 \times 10^{52} \text{ phot s}^{-1}$  (Smith et al. 1987). OB star counts around 30 Dor (*e.g.*, Parker 1993) could well underestimate the total ionizing flux by a substantial factor. Kennicutt et al. (1995) suggest that fully one third of the ionizing radiation in the LMC arises from within  $0.5^\circ$  of 30 Dor. The ground-based results may suffer from crowding which means that the total number of stars is underestimated.

We now test whether the Magellanic HI Bridge can constrain the escape fraction of UV photons from the Magellanic Clouds. Fig. 6 shows one such model prediction for the Bridge. Fujimoto & Sofue (1976) give specific positions for the LMC and SMC in Galactic coordinates. Here, we take the total ionizing flux from the LMC to be  $1 \times 10^{52} \text{ phot s}^{-1}$  and the SMC to be an order of magnitude smaller. For both galaxies, we assume that 15% of the UV escapes. The expected level in the Bridge is of order 50–100 mR, an order of magnitude higher than levels produced by the Galaxy at that large polar angle.

There are two published claims of  $H\alpha$  in the Magellanic Bridge. Johnson, Meaburn & Osman (1982) claim to see diffuse  $H\alpha$  across the entire HI bridge extending over  $30^\circ$  or more at an observed surface brightness of  $8 \text{ R} \pm 4 \text{ R}$ . Marcelin, Boulesteix & Georgelin (1985) detected the Shapley wing of the SMC in  $H\alpha$  at the level of 4 R. These  $H\alpha$  detections, which are partly confirmed by the UKST  $H\alpha$  survey (Zealey 2001, personal communication), are more than an order of magnitude stronger than expected in our simple model proposed. It seems that some of the bright  $H\alpha$  regions arise from embedded UV sources, *e.g.*, UV-bright stars in the Shapley wing. However, this does not appear to be the explanation for recent detections of bright  $H\alpha$  along the Magellanic Stream (Weiner & Williams 1996; Weiner et al. 2001, these proceedings).

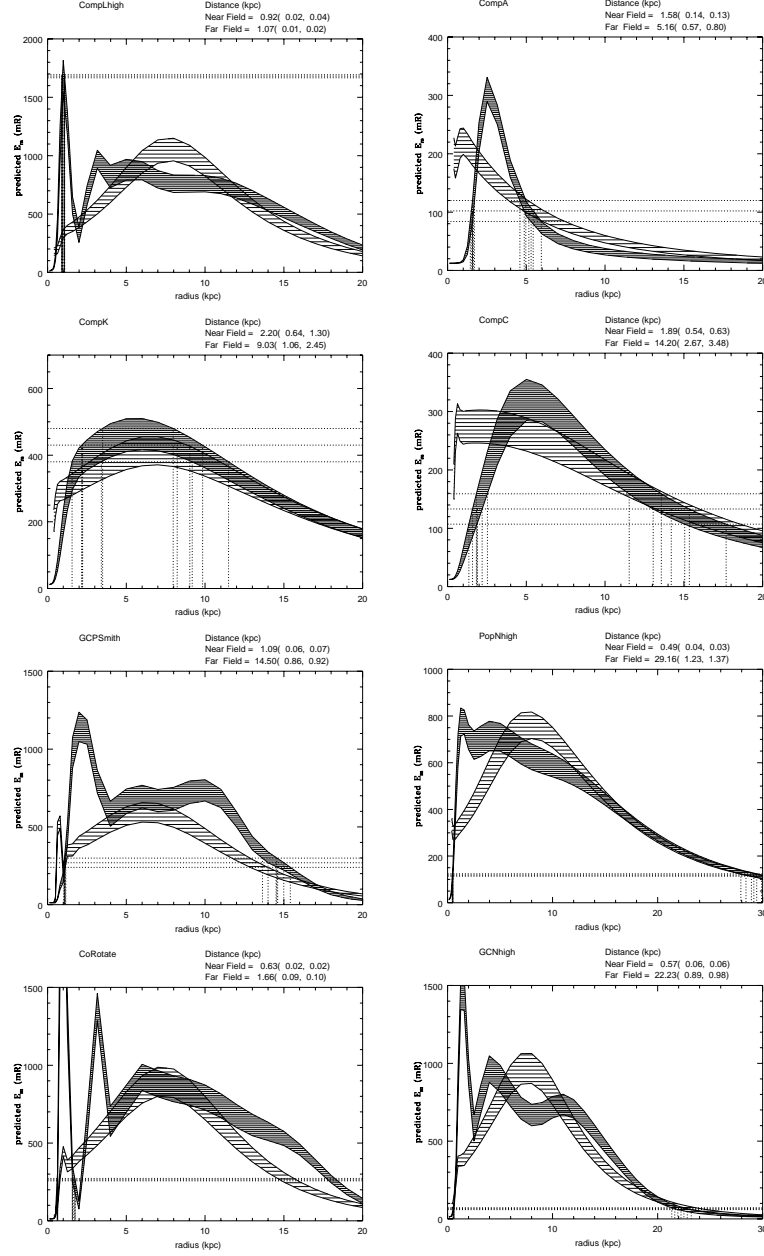


Figure 5. Predicted emission measures along the radius vector to 8 HVCs. The densely shaded band arises from the dusty spiral disk model averaged over different cloud orientations; the lighter shaded band is for a dusty exponential disk. The horizontal lines show the average and range of emission measures for the modelled position on the cloud. The vertical lines show where the horizontal lines intersect the model. For the spiral model, there is almost always a near-field and a far-field solution although low latitude vectors can produce multiple solutions.

Since the Magellanic Stream passes directly over the South Galactic Pole (illustrated in Fig. 7), BM99 had hoped this would constrain  $\hat{f}_{\text{esc}}$  from the Galaxy but their original model underestimates the required flux by at least a factor of 5. Weiner et al. (2001) claim detections to some points of the Stream as high as 1 R. The Galaxy fails to produce this level of ionization by at least an order of magnitude. The expected H $\alpha$  levels produced by the Galaxy are shown in Fig. 8 where we also show the additional contribution from the LMC. Since the LMC and much of the Stream lie close to  $Y = 0$ , the model predictions are given in this plane. Bland-Hawthorn & Putman (2001) discuss various dynamical scenarios which may account for the bright Stream detections.

In summary, the Magellanic Stream poses a clear problem for the H $\alpha$  distance method since, in a few locations, it appears to be an order of magnitude brighter than predicted by the model. The Magellanic Bridge is also H $\alpha$  bright in places, but this may be due to internal UV sources. However, the HVCs appear to be broadly consistent with the spiral arm ionization model, and we find that most HVCs detected to date are scattered throughout the halo up to distances of 50 kpc from the Sun. Our suspicion is that most of the HVCs, like the Magellanic Bridge and the Magellanic Stream, result from galaxy interactions, specifically dwarf galaxies disrupted by the Galaxy. An interesting prospect that we have been investigating with B.K. Gibson is that some of the HVCs have been dislodged from the outer disk due to the disruptive passage of a nearby dwarf. There are several observations which support this: (i) the metallicities are consistent with the outer disk; (ii) the outer HI disk looks highly disturbed (Burton & Te Lintel Hekkert 1986); (iii) in some instances the HVCs show continuity in velocity with the outer disk (*e.g.*, Gibson et al. 2001); and (iv) the H $\alpha$  distances place many of the clouds on 10 kpc scales. We have begun to carry out hydrodynamical simulations in order to test this idea further.

## References

- Bica, E. et al. 1996, A&A, 313, 405  
 Binette, L. et al. 1994, A&A, 292, 13  
 Bland-Hawthorn, J. et al. 1998, MNRAS, 299, 611  
 Bland-Hawthorn, J. & Maloney, P.R. 1999*b*, ASP Conf. 166, In Stromlo Workshop on HVCs, eds. B.K. Gibson & M.E. Putman, 212  
 Bland-Hawthorn, J. & Maloney, P.R. 1999, ApJ, 510, L33 (BM99)  
 Bland-Hawthorn, J. & Putman, M.E. 2001, In Gas & Galaxy Evolution, eds. Hibbard, Rupen & van Gorkom, 240, 369–382 (astro-ph/0110043).  
 Blitz, L., Spergel, D. N., Teuben, P. J., Hartmann, D. & Burton, W.B. 1999, ApJ, 514, 818  
 Burton, W.B. & Te Lintel Hekkert, P. 1986, A&AS, 65, 427  
 Braun, R. & Burton, W.B. 2000, A&A, 354, 853  
 Cianci, S. 2001, PhD, Sydney University  
 Domgörgen, H. & Mathis, J.S., 1994, ApJ, 428, 647  
 Dwek, E. et al. 1995, ApJ, 445, 716

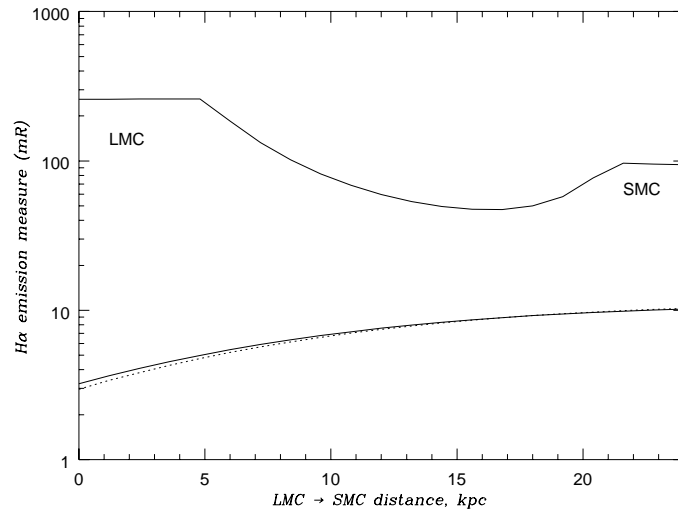


Figure 6. The predicted  $H\alpha$  emission measure along the Magellanic Bridge in units of  $\log(mR)$ . The LMC is to the left and the SMC is to the right. The upper curve is due to escaping radiation from the Magellanic Clouds. The lower curves are due the dusty exponential and spiral disks ( $\tau_{LL} = 2.8$ ).

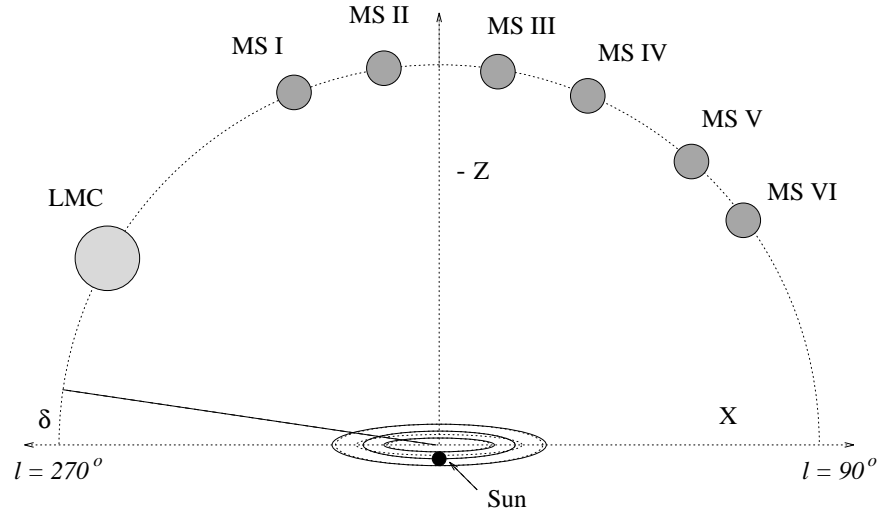


Figure 7. An illustration of the LMC and the dominant clouds in the Magellanic Stream (Mathewson & Ford 1984) projected onto the Galactic  $X$ - $Z$  plane. The orbit of the Stream lies closer to the Great Circle whose longitude is  $l = 285^\circ$ . We ignore small projection errors resulting from our vantage point at the Solar Circle. The angle  $\delta$  is measured from the negative  $X$  axis towards the negative  $Z$  axis where  $\delta = -b$  ( $0^\circ \leq \delta \leq 90^\circ$ ) and  $\delta = b + 180^\circ$  ( $90^\circ \leq \delta \leq 180^\circ$ ).

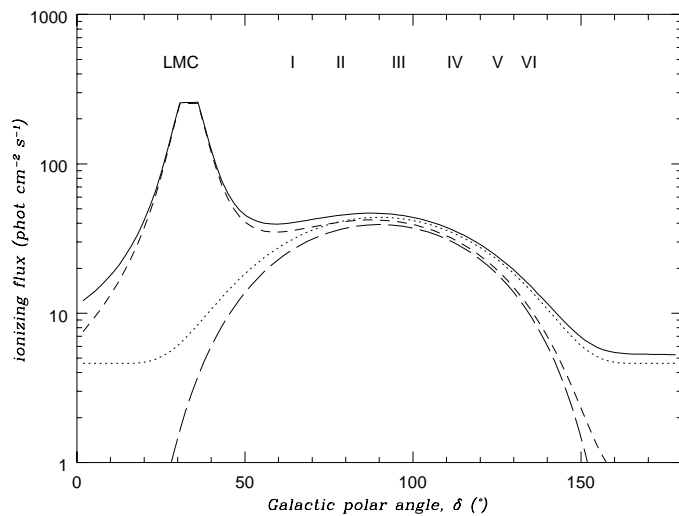


Figure 8. The predicted  $H\alpha$  emission measure along the Stream as a function of  $\delta$  (Fig. 7) in units of  $\log(\text{mR})$ . The cloud positions are illustrated in Fig. 7. All curves show the ionizing influence of the Galaxy ( $\tau_{LL} = 2.8$ ). The short dashed curve includes the contribution of the LMC; the dotted curve includes the contribution of a UV-bright stellar bulge. The solid curve includes the effect of the LMC and a stellar bulge.

- Fujimoto, M. & Sofue, Y. 1976, *A&A*, 47, 263
- Glazebrook & Bland-Hawthorn, J. 2001, *PASP*, 113, 197
- Greggio, L. & Renzini, A. 1999, *Mem. Soc. Astron. Ital.*, 70, 691
- Haffner, L.M., Reynolds, R.J. & Tufte, S.L. 1999, *ApJ*, 523, 223
- Haffner, L.M., Reynolds, R.J. & Tufte, S.L. 2001, *ApJ*, 556, L33
- Israel, F.P. & Koornneef, J. 1979, *ApJ*, 230, 390
- Johnson, P.G., Meaburn, J. & Osman, A.M.I. 1982, *MNRAS*, 198, 985
- Kennicutt, R.C. et al. 1995, *AJ*, 109, 594
- Klypin, A., Kravtsov, A.V., Valenzuela, O. & Prada, F. 1999, *ApJ*, 522, 82
- Lockman, F.J. 1984, *ApJ*, 283, 90
- Lyne, A.G., Manchester, R.N. & Taylor, J.H. 1985, *MNRAS*, 213, 613
- Macchetto, F. et al. 1996, *A&AS*, 120, 463
- Manchester, R.N. & Taylor, J.H. 2001, *Pulsars* (W.H. Freeman: San Francisco).
- Marcelin, M., Boulesteix, J. & Georgelin, Y. 1985, *Nat*, 316, 705
- Mathewson, D.S. & Ford, V.L. 1984, in *Structure and Evolution of the Magellanic Clouds*, *IAU Symp.*, 108, 125
- McGee, R.X., Brooks, S.W. & Batchelor, R.A. 1972, *Aust. J. Phys.*, 25, 581
- Moore, B., Ghigna, S., Governato, F., Lake, G., Quinn, T., Stadel, J. & Tozzi, P. 1999, *ApJ*, 524, L19
- Nordgren, T.E., Cordes, J.M. & Terzian, Y. 1992, *AJ*, 104, 1465
- O'Connell, R.W. 1999, *ARAA*, 37, 603
- Ortiz, O. & Lepine, J.R.D. 1993, *A&A*, 279, 90
- Parker, J.W. 1993, *AJ*, 106, 560
- Putman, M.E. 2000, PhD, Australia National University
- Reynolds, R.J. 1984, *ApJ*, 282, 191
- Reynolds, R.J. 1989, *ApJ*, 345, 811
- Reynolds, R.J. & Tufte, S.L. 1995, *ApJ*, 439, L17
- Reynolds, R.J., Haffner, L.M. & Tufte, S.L. 1999, *ApJ* 525, L21
- Ryans, R.S.I. et al. 1997, *MNRAS*, 289, 83
- Smith, A.P., Cornett, D.H., & Hill, R.S. 1987, *ApJ*, 320, 609
- Taylor, J.H. & Cordes, J.M. 1993, *ApJ*, 411, 674
- Tufte, S.L., Reynolds, R.J. & Haffner, L.M. 1998, *ApJ*, 504, 773
- van Woerden, H. et al. 1999, *Nat*, 400, 138
- Wakker, B.P. & van Woerden, H. 1991, *A&A* 250, 509
- Wakker, B.P. & van Woerden, H. 1997, *ARAA*, 35, 217
- Wakker, B.P. 2001, *ApJS*, in press (astro-ph/0102147)
- Walborn, N.R. 1984, in *Structure and Evolution of the Magellanic Clouds*, *IAU* 108, 243
- Weiner, B.J. & Williams, T.B. 1996, *AJ*, 111, 1156
- Weiner, B.J., Vogel, S.N. & Williams, T.B. 2001, these proceedings(astro-ph/0109055)



- Wyse, R.F.G. 1999, ASP Conf. Ser. 165: The Third Stromlo Symposium: The Galactic Halo, 1
- Zhao, H. 1996, MNRAS, 283, 149
- Zurita, A. et al. 2001, A&A, in press (astro-ph/0108135)
- Zwaan, M. & Briggs, F. 2000, A&A, 530, L61